Mater. Res. Soc. Symp. Proc. Vol. 1282 © 2011 Materials Research Society
DOI: 10.1557/opl.2011.447

Focused Ion Beam Milling of Crystalline Diamonds

Rustin Golnabi[1], Won I. Lee[1], Deok-Yang Kim[1], and Glen R. Kowach[2]
[1] Bergen County Academies, 200 Hackensack Avenue,
Hackensack, NJ 07601, U.S.A.
[2] Department of Chemistry, The City College of New York, 160 Convent Avenue,
New York, NY 10031, U.S.A.

ABSTRACT

Recently, a wide range of new applications of diamond materials such as spintronics, field emission, and bio-sensing have been proposed. These applications often require the precise patterning of diamonds, which is not trivial because diamonds are the hardest materials known in nature. Among various patterning techniques, the focused ion beam milling method has been proven to provide flexibility as well as high resolution in the pattern design. In this study, a focused beam of 30 kV Ga^+ ions was utilized to create sub-micrometer size patterns out of crystalline diamonds. The sputtering rate, re-deposition, and surface roughening of diamond structure have been closely monitored with various milling parameters during the milling process. Our study revealed a low milling yield of 0.02 μm^3/nC, high Ga content re-deposition, and the formation of sub-micron scale terracing on the sidewall of patterned diamonds.

INTRODUCTION

Focused ion beam (FIB) milling has recently found many applications in a variety of nanoscale patterning and fabrication. It is often utilized in the maskless micromachining and patterning of materials [1], especially metal alloys, due to the high level of precision provided by the technique [2]. Furthermore, the application of FIB to microfabrication has become increasingly popular, due to the lack of necessity for a mask, high resolution to microscale features, and versatility in numerous geometric patterns [3]. In particular, this study involves the use of gallium (Ga^+) ion milling, commonly used in FIB systems. Previously, gallium FIB has also been used in ion beam-induced deposition with various precursors [4].

For diamond, one of the only viable ways to fabricate microscale patterns is by focused ion beam. Recently, several applications of diamond materials such as spintronics, field emission, and bio-sensing have been studied [5-7]. These functions often require the precise pattering of diamond, which is difficult because diamond is such a hard material; consequently, FIB is one of the few methods by which diamond can be precisely patterned [8]. However, a number of additional effects makes the process rather unpredictable and arduous. Re-deposition of both the milled carbon and Ga^+ ions from the FIB results in unintended structural formations, while nano-terracing ("ripple") effects often disrupt clean milling patterns [9].

Consequently, it is necessary to determine methods by which to minimize such detrimental effects for the efficient milling of diamond materials for a number of significant applications. In this study, several varying conditions are used in milling diamond in order to observe the effects of re-deposition and nano-terracing on single-crystal milling, as well as determine the area-to-current relationships in diamond patterning by FIB.

EXPERIMENT

The single crystal (110) diamond was gold-coated using a Denton Desk IV sputter coater to prevent charging issues before being ion-milled with a FEI Quanta 3D 200 Dual Beam, which used Si as the material file. The thickness of a gold film on the diamond sample was estimated to be 3 nm based on the blue color of the gold film simultaneously deposited on the glass slide. The ion beam source was 30 kV Ga^+ with various ion beam currents as described in the result and discussion section. Imaging and analysis of the milled diamond sample was completed with either the same instrument utilizing the scanning electron microscope (SEM) column or a Zeiss Supra 55VP field emission SEM with energy dispersive X-ray spectroscopy (EDX), used at the City College of New York. Computational analysis of the images was performed using ImageJ software.

RESULTS AND DISCUSSION

Re-deposition effects & milling rate

In order to observe the effects of re-deposition, a total of 4 sequential focused ion-milling patterns (dimension settings of 1 μm x 50 μm x 50 μm; Width x Length x Depth; total run time of 900 seconds each, determined by silicon reference material file) at 20 nA were etched on the single crystal diamond sample. Figure 1 shows that the width of trench got enlarged to 5 μm possibly due to large ion current and that the re-deposited materials refill the previously etched lines resulting in shallower trenches surrounding each new pattern. The re-deposition effects were observed to be widespread and reach across lengths of over 2 μm. The SEM micrograph on the right (Figure 1) reveals the inverted pyramidal cross-section of the milled trench. X-ray elemental analysis on re-deposited areas showed gallium-enriched carbon composition (Ga 6 atomic percent/Carbon 94 atomic percent from our EDX analysis).

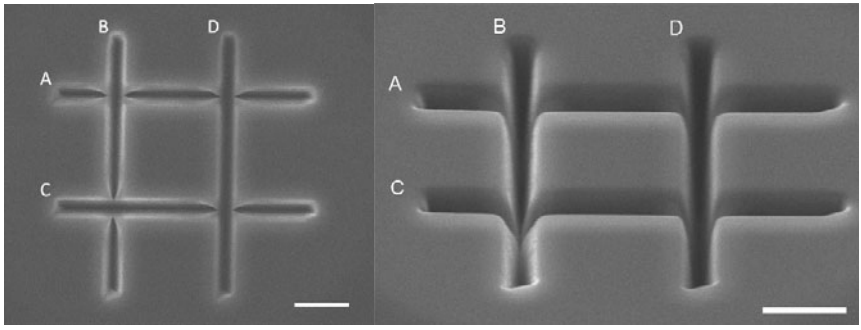

Figure 1. The linear patterns were etched sequentially, starting with line A(from left to right) at 1 μm x 50 μm x 50 μm; then line B(from top to bottom), C(from left to right), and D(from top to bottom), with identical dimensions. The scale bars in both Figures represent 10 μm.

In the Figure 2, two identical 1 μm by 5 μm rectangles at 20 nA were etched near the edge of the diamond sample, with different depth settings respectively. The depth of the left rectangle pattern was set to 50 μm (total milling time of 180 s). However, the actual depth was measured to be only about 12.3 μm (milling rate of 0.07 μm/s). The second pattern was also a 1 x 5 μm rectangle, but this time with a depth setting of 150 μm (280 seconds). The actual depth was measured to be about 13.5 μm (milling rate of 0.05 μm/s). It is likely that cone-shaped trench resulted from the re-deposition of gallium rich carbon materials as they increasingly filled both sides of the trench, therefore slowing down the etch rate. Also, it was noted that the trench with longer milling time had 50% larger width.

The average milling yield of both trenches was estimated (using inverted pyramid for left side and inverted trapezoid for right side) to be 0.02 μm^3/nC, which is significantly lower than 1.8 μm^3/nC, the number D.P. Adams quoted in [10].

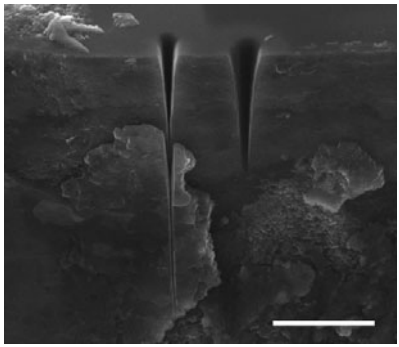

Figure 2. The trench in the left was designated a depth of 50 μm (actual depth was 12.3 μm), and width of 1 μm (actual width was 4.1 μm). The second trench in the right was set for a depth of 150 μm (actual depth was 13.5 μm), and a width of 1 μm (actual width was 6.3 μm). The scale bar represents 20 μm in length.

Milling accuracy using variable currents

To determine the effect of ion current on the milled pattern, first square patterns of 2 μm by 2 μm were etched with various ion currents of 1 nA, 3 nA, 5 nA, 7 nA, and 20 nA. The depth of the pattern was set to 20 μm for all of them (Figure 3a). In addition, the triangular patterns with same ion current conditions (Figure 3b) were milled in order to compare the effect of ion current with different pattern shape.

The shapes of milled pattern deviated considerably from the designated pattern in both square and triangle cases with increasing current. The lowest current setting of 1 nA yielded the most accurate pattern in the agreement with the desired pattern. As the current increased, the milled patterns became progressively more hexagonal in form for the square pattern. For triangular pattern, high ion current produced curved edges. Close-up SEM micrographs of square patterns were shown in the Figure 3 c, d, and e. They all revealed inverted and truncated hexagonal pyramid trenches as the one in the Figure c being the closest to the shape of truncated square pyramid. The change in the shape is expected because higher ion current may alter the

size and shape of incident ion beams. Also, possibly due to the re-deposition process, the large area difference in the etched top surface (basal plane of inverted pyramid) and the bottom surface were observed. It is noted that preferred milling directions exist in the Figure 3 c and d, but future studies are required to confirm whether they are related to the crystal orientation of the diamond crystal.

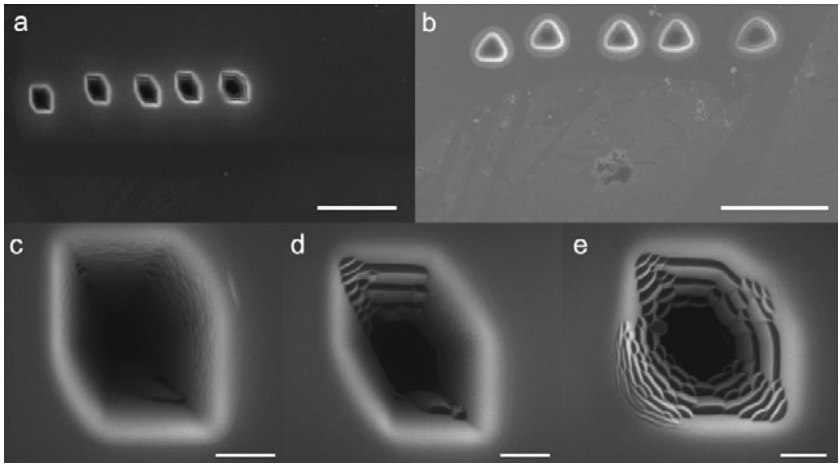

Figure 3. Scanning electron micrographs of a) square (2 μm x 2 μm x 20 μm) patterns at varying currents (from left to right: 1 nA, 3 nA, 5 nA, 7 nA, and 20 nA); b) triangular (2 μm x 1.5 μm x 20 μm) at the aforementioned currents; c) square pattern at 1 nA; d) square pattern at 5 nA; and e) square pattern at 20 nA, with the most extensive nano-terracing, as observed. Scale bars in *a* and *b* represents 10 μm, while scale bars in *c*, *d*, and *e* represent lengths of 1 μm. Notice the slight magnification difference in the Figure *c*, *d*, and *e*.

In addition, it is evident that higher ion current induces large sidewall roughness on the trenches. Again, the lowest current setting of 1 nA yielded the smoothest sidewall. The close examination of previously milled trenches in the Figure 1 and Figure 2 also confirmed the existence of large surface roughness induced by the Ga^+ ion current of 20 nA (Figure 4).

Figure 5 depicts the area percents of etched top and bottom surfaces of the single crystal diamond to the expected area by design (e.g. 2 x 2 μm^2 for the square pattern). Both the top surface areas and bottom surface areas increased linearly with the ion current at lower range from 1 nA to 7 nA. However, the increase in area percent for the bottom surfaces appears to saturate at around 7 nA, while the top surface areas continues increasing linearly with ion current. Both square and triangle pattern showed similar trend.

Significantly, the top surface areas for all patterns exceeded the expected number with even the lowest current (1 nA) trial producing about 150% for the square pattern. Interestingly, the enlargement of triangular pattern was even more pronounced even at the lowest current (240%). Furthermore, strong disparity existed between the area percents of the top and bottom surfaces. At the lowest current, the top area was almost an order of magnitude greater than the bottom surface area in case of the square pattern. As the current was increased, the disparity between the

two surface areas rose as well. Consequently, it is reasonable to expect that the FIB milling had resulted in the formation of a conically-structured hole, with greater depth resulting, as expected, from the use of a higher current.

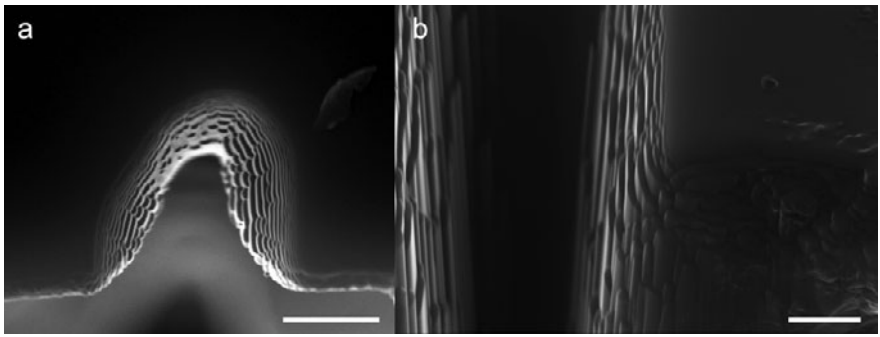

Figure 4. Nano-terraces on the sidewalls of milled single-crystal diamond (ion beam current of 20 nA). a) Top view of the 150 μm-depth hole in Figure 2 (right trench); b) Side view of the intersection of trenches A and B in Figure 1. Scale bars represent 3 μm in *a* and 1 μm in *b*.

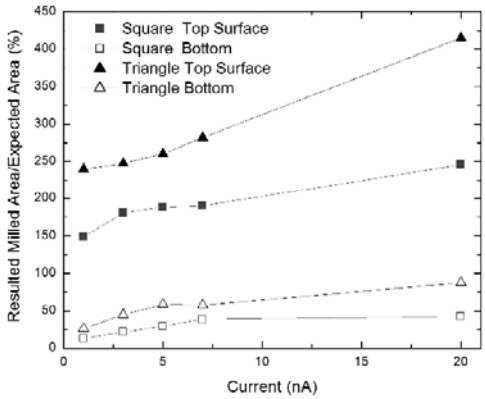

Figure 5. Relationship between the surface areas of the square patterns and triangle patterns per each current value, where the top surface area indicates the milled area of diamond surface, and the bottom surface area indicates the milled area at the bottom of the trench.

CONCLUSIONS

Milling with the Ga^+ focused ion beam and subsequent analysis of generated patterns yielded following conclusions regarding the accuracy and parameters of focused ion beam

milling on single-crystal diamond. First, FIB milling tends to produce conically-structured holes in diamond, primarily because gallium-based carbon re-deposition takes place. It is hypothesized that the re-deposition increasingly fills the trench as the milling process continues. Our elemental analysis on the re-deposited area showed large gallium content in the carbon, which may not be easily removed. Secondly, the increase in the ion current resulted in a less accurate design possibly due to much larger and distorted ion beam size. At the same time, higher ion current induces greater nanosize-terracing effects and rougher sidewalls of the pattern. Because of the undesirability of both of these effects, milling at lesser currents (i.e. 1 nA) would be optimal for more accurate shapes, sizes, and edges. Of course, the drawback of using such a low current is the protracted length of time that it requires compared to milling at higher currents.

It was found that a lowest current is best for accuracy; re-deposition and sputtering must be taken into full consideration during the milling of such a hard material as diamond, and these effects unerringly result in conically-structured holes upon milling. Because of the number of disadvantages presented by high ion current during FIB milling process as discussed, future research on the diamond milling should be directed towards utilizing reactive gas vapor assisted milling of single crystal diamonds [10].

ACKNOWLEDGMENTS

We are grateful to Dr. Howard Lerner, Superintendent of the Bergen County Technical Schools District, and Ms. Andrea Sheridan, Assistant Superintendent of the Bergen County Technical Schools District for their support of the nanotechnology research program. We also thank Mr. Russell Davis, Principal of the Bergen County Academies for his support and encouragement. Finally, we appreciate the assistance of David Becker, Alyssa Calabro and Craig Queenan, Nano-Structural Imaging Lab staff members at our school district. The FEI dual beam equipment at Bergen County Academies was purchased with Carl D. Perkins grant. The Zeiss Supra SEM at the City College of New York was obtained through National Science Foundation – Major Research Instrumentation grant (#0923084).

REFERENCES

[1] S. Reyntjens and R. Puers, J. Micromech. Microeng., 11, 287 (2001)
[2] D. P. Adams, M. J. Vasile, G. Benavides, and A. N. Campbell, Precis. Eng., 25, 107 (2001)
[3] A. A. Tseng, J. Micromech. Microeng., 14, R15 (2004)
[4] E.S. Sadki, S. Ooi, and K. Hirata, Appl. Phys. Lett., 85, 6206 (2004)
[5] R. Hanson, O. Gywat, and D. D. Awschalom, Phys. Rev. B, 74, 1203 (2006)
[6] M. W. Geis, J. C. Twichell, J. Macaulay, and K. Okano, Appl. Phys. Lett., 67, 1328 (1995)
[7] A. Härtl, E. Schmich, J. A. Garrido, J. Hernando, S. C. R. Catharino, S. Walter, P. Feulner, A. Kromka, D. Steinmüller, and M. Stutzmann, Nat. Mater., 3, 736 (2004)
[8] A. Stanishevsky, Thin Solid Films, 398, 560 (2001)
[9] A. Datta, Y. Wu, and Y. L. Wang, Phys. Rev. B, 64, 5407 (2001)
[10] D.P. Adams, M.J. Vasile, T.M. Mayer and V.C. Hodges, J. Vac. Sci. Tech. B, 21, 2334 (2003)